Numerical Dispersion Analysis of the Unconditionally Stable 3-D ADI–FDTD Method

Fenghua Zheng and Zhizhang Chen

***Abstract*—This paper presents a comprehensive analysis of numerical dispersion of the recently developed unconditionally stable three-dimensional finite-difference time-domain (FDTD) method where the alternating-direction-implicit technique is applied. The dispersion relation is derived analytically and the effects of spatial and temporal steps on the numerical dispersion are investigated. It is found that the unconditionally stable FDTD scheme has advantages over the conventional FDTD of the Yee's scheme in modeling structures of fine geometry where a graded mesh is required. The unconditionally stable FDTD allows the use of a large time step in a region of fine meshes while maintaining numerical dispersion errors smaller than those associated with the region of coarse meshes.**

***Index Terms*—CFL stability conditions, numerical dispersion, unconditionally stable FDTD.**

I. Introduction

The finite-difference time-domain (FDTD) method is widely used to simulate transient electromagnetic-wave propagation since it is robust, fast, simple to implement, and possible to achieve the responses in a chosen frequency band with one single round of simulation [1], [2]. However, since the FDTD method is an *explicit* time-stepping technique, its time step is limited by the well-known Courant–Friedich–Lecy (CFL) stability condition [2]. As a result, the FDTD may require a large number of iterations in certain applications, especially when structures of fine geometry (such as small via) are involved.

To eliminate the CFL stability condition, implicit methods can be used. These implicit techniques, in particular, alternating-direction-implicit (ADI) methods, have been widely used in solving heat transfer problems [3], leading to various unconditionally stable finite-difference formulations for parabolic equations [4]. Very recently, such implicit techniques were introduced into the FDTD schemes for solving Maxwell's equations, resulting in an implicit unconditionally stable ADI–FDTD method [5]–[7]. In particular, a rigorous theoretical proof of the unconditional stability was presented with numerical verifications in [7]. Due to the removal of the CFL conditions, the time step used is no longer restricted by the stability conditions, but by modeling accuracy of the algorithm. One of the factors that affect the accuracy is numerical dispersion.

This paper presents the study on numerical dispersion characteristics of the unconditionally stable ADI–FDTD. An analytical formula is derived and the effects of the time and spatial steps on the numerical dispersion are investigated. An important corollary regarding the numerical dispersion errors of a graded mesh or multigrid is also presented.

II. Numerical Dispersion of the Unconditionally Stable ADI–FDTD

In this section, the dispersion of the FDTD scheme is derived by following a similar procedure described in [2].

Manuscript received October 6, 1999; revised July 26, 2000. This work was supported by the Natural Sciences and Engineering Research Council of Canada.

The authors are with the Department of Electrical and Computer Engineering, Dalhousie University, Halifax, NS, Canada B3J 2X4 (e-mail: z.chen@dal.ca).

Publisher Item Identifier S 0018-9480(01)03320-8.

The relationship between the field components at the $(n+1)$th time step and the nth time step in the spatial spectral domain were obtained in [7]

$$\mathbf{F}^{n+1} = \Lambda \mathbf{F}^{n} \tag{1}$$

where Λ is shown in the first equation at the bottom of the following page, with

$$\begin{aligned}
W_\alpha &= \frac{\Delta t}{\Delta \alpha} \cdot \sin\left(\frac{k_\alpha \Delta \alpha}{2}\right) \\
Q_\alpha &= 1 + \frac{W_\alpha^2}{\mu\varepsilon} \\
\alpha &= x,\ y,\ z \\
W &= W_x W_y W_z \\
A_1 &= \mu^3\varepsilon^3 + \mu^2\varepsilon^2\left(W_x^2 - W_y^2 - W_z^2\right) + W_x^2 W_y^2 W_z^2 \\
A_2 &= \mu^3\varepsilon^3 + \mu^2\varepsilon^2\left(W_y^2 - W_z^2 - W_x^2\right) + W_x^2 W_y^2 W_z^2 \\
A_3 &= \mu^3\varepsilon^3 + \mu^2\varepsilon^2\left(W_z^2 - W_x^2 - W_y^2\right) + W_x^2 W_y^2 W_z^2 \\
B_1 &= \mu\varepsilon\left(W_x^2 W_y^2 - W_y^2 W_z^2 - W_z^2 W_x^2\right) \\
B_2 &= \mu\varepsilon\left(W_y^2 W_z^2 - W_z^2 W_x^2 - W_x^2 W_y^2\right) \\
B_3 &= \mu\varepsilon\left(W_z^2 W_x^2 - W_x^2 W_y^2 - W_y^2 W_z^2\right) \\
D_1 &= W_y\left(W_x^2 W_z^2 - \mu^2\varepsilon^2\right) \\
D_2 &= W_z\left(W_y^2 W_x^2 - \mu^2\varepsilon^2\right) \\
D_3 &= W_x\left(W_z^2 W_y^2 - \mu^2\varepsilon^2\right).
\end{aligned}$$

Here, Λ is a 6×6 matrix that contains $k_x\Delta x$, $k_y\Delta y$, and $k_z\Delta z$. k_x, k_y, and k_z are the spatial frequencies along the x- y-, and z-directions, respectively. Δx, Δy, and Δz are the spatial steps. $\mathbf{F}$ is a vector that contains all six field components in the spatial spectral domain

$$F^n = \left[E_x^n \;\; E_y^n \;\; E_z^n \;\; H_x^n \;\; H_y^n \;\; H_z^n\right]^T. \tag{2}$$

Now, assume the fields to be a monochromatic wave with angular frequency ω

$$E_\alpha^n = E_\alpha e^{j\omega\Delta t n} \quad H_\alpha^n = H_\alpha e^{j\omega\Delta t n}, \qquad \alpha = x,\ y,\ z. \tag{3}$$

Equation (1) then becomes

$$(e^{j\omega\Delta t}\mathbf{I} - \Lambda)\mathbf{F} = \mathbf{0} \tag{4}$$

where $\mathbf{I}$ is a 6×6 identity matrix and $\mathbf{F}$ is the field vector defined by

$$\mathbf{F}^n = \mathbf{F} e^{j\omega\Delta t n}. \tag{5}$$

For a nontrivial solution of (4), the determinant of the coefficient matrix should be zero as follows:

$$\det\left(e^{j\omega\Delta t}\mathbf{I} - \Lambda\right) = 0. \tag{6}$$

With the help of Maple V5.0, the above equation can be simplified, as shown in (7), at the bottom of the following page, which is the dispersion relationship of the unconditionally stable ADI–FDTD method.

III. Numerical Dispersion Results and Discussion

Several aspects of the numerical dispersion studies are performed in this aspect. They include: 1) the effect of the propagation direction on the dispersion; 2) the effect of the large time step on the dispersion; 3) the dispersion on the $k_x - k_y$ plane; and 4) an important corollary regarding the graded mesh or multigrid.

1) Effect of the Propagation Direction on the Dispersion: Suppose that a wave propagating at angle ϕ and θ is in the spherical coordinate system. Then, $k_x = k\sin\theta\sin\phi$, $k_y = k\sin\theta\cos\phi$, and $k_y = k\cos\theta$. By substituting them into dispersion relation (7), numerical phase velocity $v_p = \omega/k$ can be solved numerically. For simplicity, uniform cells are considered here ($\Delta x = \Delta y = \Delta z = \delta$).

Fig. 1 shows the variations of the numerical phase velocity with the wave propagation angles with a time step smaller than the CFL limit. It is seen that the numerical phase velocity error reaches minimum at 45° and maximum at 0° and 90°. This represents a numerical anisotropy that is inherent in the FDTD algorithm. In comparison with the dispersion errors of the conventional FDTD method (not shown due to space limitation), one can find that the difference between the two methods is very small. In general, below the time step defined by the CFL condition, both the unconditionally stable FDTD and the conventional FDTD present the very similar dispersion behaviors.

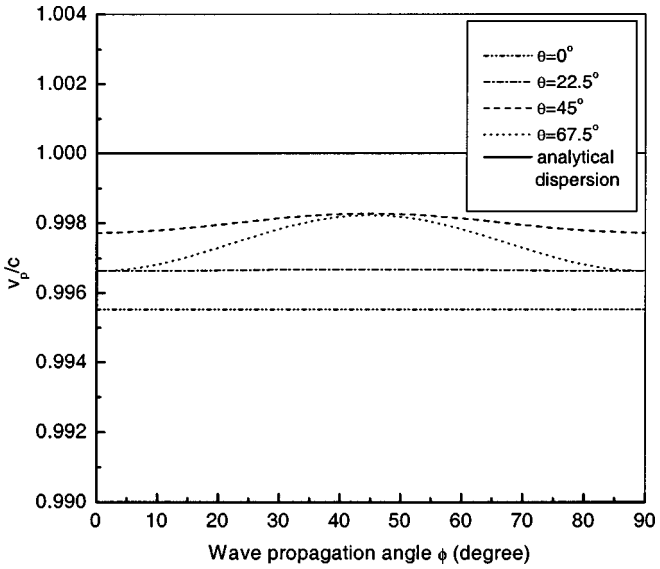

Fig. 1. Numerical phase velocity versus wave propagation angle with the unconditionally stable FDTD grid with $\delta = \lambda/20$ and $\Delta t = \delta/c/5$.

2) Effect of the Large Time Step on the Numerical Dispersion: Since the time step in the unconditionally stable FDTD scheme is no longer restricted by the CFL condition, it is important and meaningful to see how a large time step impacts on numerical dispersion, in particular, for a time step larger than the CFL limit. In our studies, two different time steps are selected: $\Delta t = \delta/c$ ($\sqrt{3}\times$ the CFL limit) and $\Delta t = 1.5\delta/c$ (2.6× the CFL limit). In both cases, a uniform spatial discretization $\delta = \lambda/20$ was used.

Figs. 2 and 3 illustrate how time steps affect the numerical phase velocity. It is obvious that the curves in the two figures basically have the same shape. However, the dispersion errors increase when the time steps increase. With the time step of 2.6 times of the CFL limit (see Fig. 3), the error reaches 2.2%. This is an indication that the time step cannot be made too large. Its selection depends very much on the accuracy level that can be tolerated by a user or modeler. Our numerical experience suggests that the time steps could be made up to four times larger than that of the conventional FDTD with acceptable accuracy when a spatial resolution $\delta = \lambda/10 \sim \lambda/20$ is used.

3) Dispersion on the k_x–k_y-Plane: In order to view dispersion characteristics more closely and precisely, the dispersion is shown on the cut of the k_x–k_y-plane ($\theta = 90°$, $k_z = k\cos\theta = 0$).

Fig. 4 shows the numerical dispersion characteristics obtained for a large time step. In this figure, three different mesh sizes are considered: coarse ($\delta = \lambda/10$), normal ($\delta = \lambda/20$), and fine ($\delta = \lambda/40$). In comparison with Fig. 1 for a smaller time step, Fig. 4 shows larger errors for a large time step. Note that, for the coarse grid, the errors are larger than the errors for the fine mesh. The errors for the coarse mesh can reach 10%. However, for the fine mesh, the errors remain small.

4) Important Corollary: The results shown in Fig. 4 have an important implication in terms of the application of the unconditionally stable

$$\Lambda = \begin{bmatrix} \frac{A_1+B_1}{Q_xQ_yQ_z} & \frac{2\mu\varepsilon W_xW_y}{Q_xQ_y} & \frac{2\mu\varepsilon W_xW_z}{Q_yQ_z} & \frac{-2j\mu W}{Q_xQ_y} & \frac{2j\mu^2\varepsilon W_z}{Q_yQ_z} & \frac{2j\mu D_1}{Q_xQ_yQ_z} \\ \frac{2\mu\varepsilon W_yW_x}{Q_zQ_x} & \frac{A_2+B_2}{Q_xQ_yQ_z} & \frac{2\mu\varepsilon W_yW_z}{Q_yQ_z} & \frac{2j\mu D_2}{Q_xQ_yQ_z} & \frac{-2j\mu W}{Q_yQ_z} & \frac{2j\mu^2\varepsilon W_x}{Q_zQ_x} \\ \frac{2\mu\varepsilon W_zW_x}{Q_zQ_x} & \frac{2\mu\varepsilon W_zW_y}{Q_xQ_y} & \frac{A_3+B_3}{Q_xQ_yQ_z} & \frac{2j\mu^2\varepsilon W_y}{Q_xQ_y} & \frac{2j\mu D_3}{Q_xQ_yQ_z} & \frac{-2j\mu W}{Q_zQ_x} \\ \frac{-2j\varepsilon W}{Q_xQ_z} & \frac{2j\varepsilon D_2}{Q_xQ_yQ_z} & \frac{2j\mu\varepsilon^2 W_y}{Q_yQ_z} & \frac{A_1+B_3}{Q_xQ_yQ_z} & \frac{2\mu\varepsilon W_xW_y}{Q_yQ_z} & \frac{2\mu\varepsilon W_zW_x}{Q_zQ_x} \\ \frac{2j\mu\varepsilon^2 W_z}{Q_zQ_x} & \frac{-2j\varepsilon W}{Q_yQ_x} & \frac{2j\varepsilon D_3}{Q_xQ_yQ_z} & \frac{2\mu\varepsilon W_xW_y}{Q_xQ_y} & \frac{A_2+B_1}{Q_xQ_yQ_z} & \frac{2\mu\varepsilon W_yW_z}{Q_zQ_x} \\ \frac{2j\varepsilon D_1}{Q_xQ_yQ_z} & \frac{2j\mu\varepsilon^2 W_x}{Q_xQ_y} & \frac{-2j\varepsilon W}{Q_zQ_y} & \frac{2\mu\varepsilon W_zW_x}{Q_xQ_y} & \frac{2\mu\varepsilon W_yW_z}{Q_yQ_z} & \frac{A_3+B_2}{Q_xQ_yQ_z} \end{bmatrix}$$

$$\sin^2(\omega\Delta t) = \frac{4\mu\varepsilon\left(\mu\varepsilon W_x^2 + \mu\varepsilon W_y^2 + \mu\varepsilon W_z^2 + W_x^2W_y^2 + W_y^2W_z^2 + W_z^2W_x^2\right)big(\mu^3\varepsilon^3 + W_x^2W_y^2W_z^2\right)}{\left(\mu\varepsilon + W_x^2\right)^2\left(\mu\varepsilon + W_y^2\right)^2\left(\mu\varepsilon + W_z^2\right)^2} \tag{7}$$

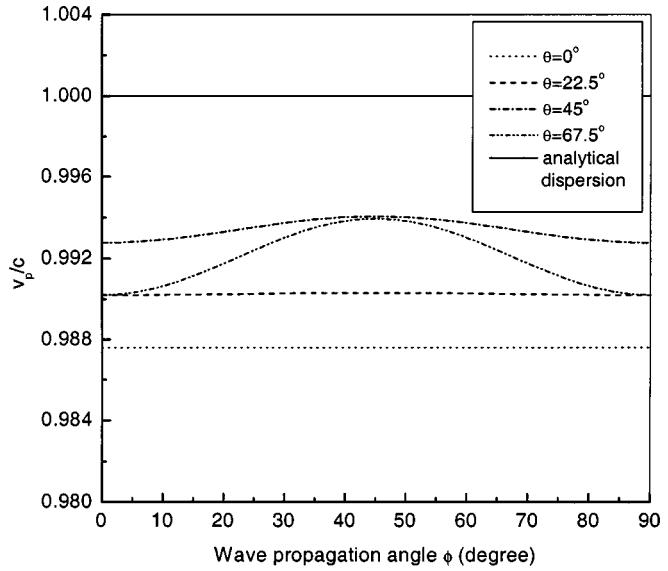

Fig. 2. Numerical phase velocity versus wave propagation angle with the unconditionally stable FDTD grid with $\delta = \lambda/20$ and $\Delta t = \delta/c$ (1.73× the CFL limit).

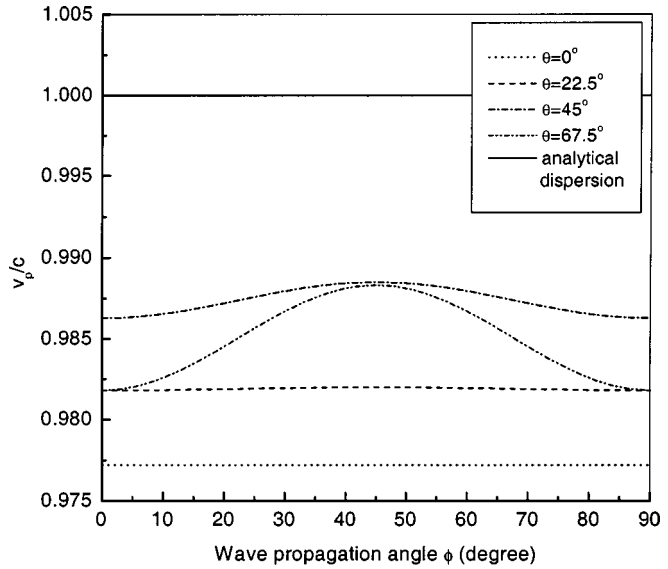

Fig. 3. Numerical phase velocity with wave propagation angle with the unconditionally stable FDTD grid with at $\delta = \lambda/20$ and $\Delta t = 1.5\delta/c$ (2.6× the CFL limit).

ADI–FDTD to FDTD graded meshes or multigrids. With the conventional FDTD, a small time step has to be taken due to the CFL stability condition applied in the refined mesh region. The overall computation time is then increased. However, with the unconditionally stable FDTD, the time step can be chosen large even for the fine mesh. Therefore, the computation time is reduced. In the following, a quantitative analysis of the dispersion error bound of a locally refined mesh is provided in reference to the dispersion of the nonrefined mesh (i.e., the coarse mesh).

Suppose a solution domain is discretized with graded meshes. Denote the overall largest coarse grid size as δ_a and the refined grid size as δ_l. The ratio of the coarse grid size to the local grid size is defined as

$$r = \frac{\delta_a}{\delta_l} \tag{8}$$

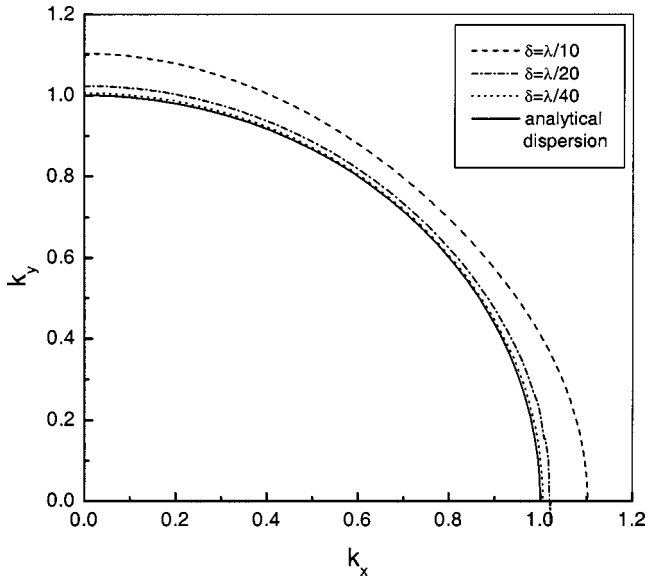

Fig. 4. Dispersion characteristics of different mesh sizes at time step $\Delta t = 1.5\delta/c$ (2.6× the CFL limit).

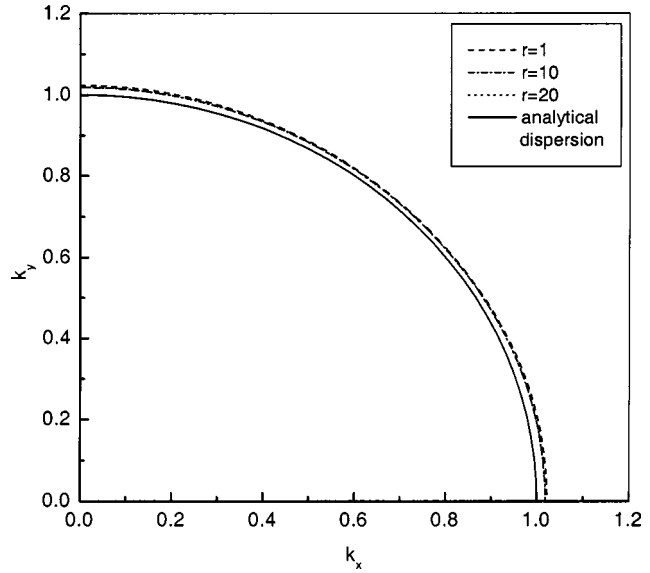

Fig. 5. Dispersion characteristics of different s at time step $\Delta t = 1.5\delta_a/c$ ($2.6r\times$ the Δt_{CFL}).

and the CFL condition stipulates that

$$\Delta t_{\mathrm{CFL}} = \delta_l/c/\sqrt{3}. \tag{9}$$

Fig. 5 shows the dispersion with $\Delta t = 1.5\delta_a/c$ ($2.6r\times$ the Δt_{CFL}) of the refined meshes of $r = 1$ (no mesh refinement), $r = 10$ (moderately refined mesh), and $r = 20$ (highly refined meshes), respectively.

As can be seen, the numerical dispersion errors decrease as r increases. That is, for a finer mesh, the dispersion is smaller. This leads to an important corollary: in a domain discretized with graded meshes or multigrids, one can take the time step with the refined mesh $(r > 1)$ to be the same as the time step with the course mesh $(r = 1)$ as long as the dispersion errors with the coarse mesh $(r = 1)$ are negligible. In other words, Δt is only restricted by the coarse mesh size δ_a in terms of accuracy, not by the finer mesh size δ_l because the dispersion errors with the refined meshes $(r > 1)$ are always smaller than that with the coarse mesh $(r = 1)$. The number of iterations with the uncon-

ditionally stable FDTD is then reduced by $r\times$ in comparison with the conventional FDTD of the Yee's scheme.

IV. Conclusions

The numerical dispersion of the recently developed unconditionally stable ADI–FDTD scheme has been derived in an analytical form. The impacts of spatial and time steps on the numerical dispersion have been investigated. For a time step smaller than the CFL limit, the dispersion errors of the unconditionally stable FDTD is at the same level as that of the conventional FDTD. For a larger time step, however, the dispersion errors increase as the time step increases. In a region of the solution domain that requires variable meshes, the time step can be taken uniformly the same as that used for the coarse grid. The accuracy for the finer mesh will be at least the same as that for the coarse mesh. This is a unique feature with the unconditionally stable FDTD and it reduces significantly the number of iterations with the unconditionally stable FDTD.

References

[1] K. S. Yee, "Numerical solution of initial boundary value problems involving Maxwell's equations in isotropic media," *IEEE Trans. Antennas Propagat.*, vol. AP-14, pp. 302–307, May 1966.

[2] A. Taflove, *Computational Electrodynamics: The Finite-Difference Time-Domain Method*. Norwood, MA: Artech House, 1996.

[3] M. N. Ozisik, *Finite Difference Methods in Heat Transfer*. Boca Raton, FL: CRC Press, 1994.

[4] Michell and Griffith, *The Finite Difference Method in Practical Differential Equations*. New York: Wiley, 1980.

[5] T. Namiki and K. Ito, "A new FDTD algorithm free from the CFL condition restraint for a 2D-TE wave," in *IEEE AP-S Symp. Dig.*, Orlando, FL, July 1999, pp. 192–195.

[6] F. Zheng, Z. Chen, and J. Zhang, "A finite-different time-domain method without the Courant stability condition," *IEEE Microwave Guided Wave Lett.*, vol. 9, pp. 441–443, Nov. 1999.

[7] ——, "Toward the development of a three-dimensional unconditionally stable finite-difference time-domain method," *IEEE Trans. Microwave Theory Tech.*, vol. 48, pp. 1050–1058, Sept. 2000.